INNSPUB

International Journal of Biosciences | IJB |
ISSN: 2220-6655 (Print); 2222-5234 (Online)
Website: https://www.innspub.net
Email contact: info@innspub.net
Vol. 29, Issue: 4, p. 122-132, 2026

RESEARCH PAPER OPEN ACCESS

Phytochemical profile, antioxidant capacity, acetylcholinesterase inhibition and GC-MS characterization of *Myosotis sylvatica* flowers

Kier Gasga*

Natural Products Research Center, Partido State University, San Juan Bautista St., Goa, Camarines Sur, Philippines

Key words: Acetylcholinesterase, Antioxidant capacity, Flower extract, GC-MS, *Myosotis sylvatica*, Phytochemistry

Received: September 26, 2026 **Accepted:** October 06, 2026 **Published:** October 14, 2026

DOI: https://dx.doi.org/10.12692/ijb/29.4.122-132

ABSTRACT

The biological activity of *Myosotis sylvatica* flowers remains poorly characterized despite the use of the genus in edible and ornamental preparations. This study evaluated extraction yield, phenolic and flavonoid indices, antioxidant capacity, acetylcholinesterase (AChE) inhibition, and the derivatized gas chromatography-mass spectrometry (GC-MS) profile of a dried ethanolic flower extract. Three independent extraction batches were prepared from 100 g dried flowers per batch; after ethanol maceration, rotary evaporation and oven drying at 40 °C to constant mass, the extraction yield was 23.70 ± 0.275% (w/w). All quantitative assays were performed across three independent trials using separately prepared batches. Matched extract blanks were incorporated at each test concentration to correct intrinsic absorbance of the naturally colored extract. IC_{50} values refer to operational concentrations in the final assay reaction mixture or microplate well. Total phenolic content was 117.937 ± 1.074 mg gallic acid equivalents/g extract and total flavonoid content was 26.418 ± 0.278 mg quercetin equivalents/g extract. DPPH radical-scavenging activity gave an IC_{50} of 113.25 µg/mL, while ferric-reducing antioxidant power and total antioxidant capacity were 380.84 mM Fe^{2+} equivalents and 514.71 mM Trolox equivalents, respectively. AChE inhibition yielded an IC_{50} of 28.44 µg/mL compared with 0.39 µg/mL for galantamine. Derivatized GC-MS produced 44 library-matched peaks, with relevant putative annotations including γ-sitosterol, linoleic acid, syringic acid, campesterol, stigmasterol and phytol. Together, the results demonstrate a consistent antioxidant and AChE-inhibitory profile in independently prepared dried ethanolic *Myosotis sylvatica* flower extracts and provide a chemically informed basis for bioassay-guided fractionation.

***Corresponding author:** Kier Gasga ✉ kier.gasga@parsu.edu.ph
https://orcid.org/0000-0003-4979-4588

INTRODUCTION

Alzheimer's disease is a progressive neurodegenerative disorder in which cholinergic dysfunction, oxidative stress, amyloid-β accumulation, tau pathology and synaptic failure interact over a prolonged course (Knopman *et al.*, 2021; Scheltens *et al.*, 2021).

Acetylcholinesterase (AChE) remains a clinically relevant symptomatic target because inhibition of the enzyme increases acetylcholine persistence at cholinergic synapses (Hampel *et al.*, 2018; Chen *et al.*, 2022). At the same time, oxidative imbalance is deeply integrated with neurodegenerative biology, providing a rationale for natural-product screening strategies that evaluate cholinesterase inhibition together with complementary antioxidant endpoints (Butterfield and Halliwell, 2019; Cummings, 2021; Moreira *et al.*, 2022).

Plant secondary metabolites are chemically diverse sources of redox-active molecules and enzyme inhibitors. Polyphenols can act as electron or hydrogen donors and some also interact with cholinesterases, although activity is highly structure dependent and cannot be inferred from total phenolic content alone (Karim *et al.*, 2020; Işık and Beydemir, 2021; Smyrska-Wieleba and Mroczek, 2023). Consequently, integrated studies that combine broad phytochemical indices, orthogonal antioxidant assays, enzyme inhibition and chemical profiling are more informative than reliance on a single screening endpoint (Pisoschi *et al.*, 2016; Munteanu and Apetrei, 2021). Qualitative phytochemical screening likewise remains useful for documenting the distribution of major secondary-metabolite classes in ethnobotanically prioritized medicinal plants (Gasga, 2026). The genus *Myosotis* (Boraginaceae) remains comparatively underexplored in this context. Aqueous extracts of edible flowers, including *Myosotis sylvatica*, have shown antioxidant activity (Wang *et al.*, 2017), and a recent study described volatile profiling and antioxidant-related bioactivity of *Myosotis sylvatica* flowers (Aytar *et al.*, 2026). In the same genus, *Myosotis amoena* has recently been reported to contain phenolic constituents and to inhibit AChE and butyrylcholinesterase (Yapıcı *et al.*, 2025). Related Boraginaceae work on *Nonea micrantha* also demonstrates the value of combining antioxidant, anticholinesterase and GC-MS analyses (Imran *et al.*, 2017).

Comparable antioxidant-plus-GC-MS designs have also been used to characterize bioactive plant extracts, including *Spermadictyon suaveolens* extracts (Padinjarekutt and Saraf, 2024).

The present study evaluated extraction yield, total phenolic content (TPC), total flavonoid content (TFC), DPPH scavenging, ferric-reducing antioxidant power (FRAP), total antioxidant capacity (TAC), AChE inhibition and derivatized GC-MS profiling of dried ethanolic *Myosotis sylvatica* flower extract across independently prepared extraction batches. The analytical workflow incorporated concentration-matched extract blanks to correct intrinsic absorbance and expressed IC_{50} values on the basis of operational concentrations in the completed assay reaction mixture or well.

MATERIALS AND METHODS

Plant material and taxonomic authentication

Cultivated *Myosotis sylvatica* Ehrh. plants (Boraginaceae) were grown in a controlled garden at Partido State University-San Jose Campus, Camarines Sur, Philippines, using commercially obtained planting material. Mature flowers were harvested, and representative flowering material with vegetative parts was submitted to the Jose Vera Santos Memorial Herbarium, University of the Philippines Diliman, for taxonomic examination. The material was formally certified as *Myosotis sylvatica* Ehrh. (Boraginaceae).

Independent extraction batches and extraction yield

Three independent extraction batches were prepared. For each batch, 100.0 g of dried flower material was cleaned, dried in a cabinet dryer at 30–40 °C, powdered and macerated in 96% ethanol at a plant material-to-solvent ratio of 1:5 (w/v) for 60 h in the

dark with intermittent stirring. The suspension was filtered and the filtrate was concentrated by rotary evaporation at 40 °C and 120 rpm. The concentrate was then oven-dried at 40 °C until constant mass. The resulting dried ethanolic flower extract was used for all subsequent analyses.

Extraction yield for each independent batch was calculated on a dried-mass basis:

$$Extraction\ yield\ (\%) = \frac{m_{dried\ extract}}{m_{dried\ flowers}} \times 100 \quad (1)$$

where the numerator is the constant mass of the oven-dried ethanolic extract and the denominator is the 100.0 g starting mass of dried flower material.

Spectrophotometric instrumentation, intrinsic-color correction and concentration basis

Absorbance measurements for the colorimetric and microplate assays were obtained using SPECTROstar Nano microplate spectrophotometer (BMG LABTECH, Ortenberg, Germany). For all spectrophotometric assays, matched extract blanks were prepared at every tested extract concentration and processed in parallel to correct intrinsic absorbance of the naturally colored extract. Each blank contained the same extract concentration and assay matrix while omitting the reaction component required for analyte-dependent color development.

Comparable blank-correction procedures have been applied to colored botanical matrices in DPPH, aluminium-chloride flavonoid and cholinesterase assays (Yeo and Shahidi, 2019; Rattaya *et al.*, 2015; Anwar *et al.*, 2020; Kitazawa *et al.*, 2021).

The absorbance contribution of the extract was removed before calculation:

$$A_{corrected} = A_{reaction} - A_{extract\ blank} \quad (2)$$

For inhibition assays, sample and control absorbances were corrected against their respective blanks. All IC_{50} values reported in this study are based on operational extract or reference-standard concentrations in the completed reaction mixture or microplate well, not on pre-assay stock concentrations.

Total phenolic content

TPC was determined using a Folin-Ciocalteu colorimetric procedure adapted from Phuyal *et al.* (2020). A 500 µL aliquot of dried ethanolic extract solution (10 mg in 10 mL solvent; 1 mg/mL) was mixed with 2.5 mL of 10% aqueous Folin-Ciocalteu reagent and 2.0 mL of 7.5% Na_2CO_3. After incubation for 5 min at 50 °C and cooling, absorbance was measured at 760 nm. Gallic acid standards (50, 100, 150 and 300 µg/mL) were processed in parallel. A matched extract blank was used for intrinsic-color correction. TPC was calculated from the gallic-acid calibration and expressed as mg gallic acid equivalents (GAE)/g dried extract.

Total flavonoid content

TFC was measured by an aluminium chloride colorimetric method adapted from Madike *et al.* (2017). The dried extract was prepared at 5 mg in 100 mL solvent, corresponding to 50 µg/mL. A 500 µL aliquot was combined with 1.5 mL of 2% ethanolic $AlCl_3$ and incubated for 60 min before absorbance measurement at 420 nm. Quercetin standards (10–100 µg/mL) were processed under the same conditions. A matched extract blank was measured at the same extract concentration. The use of a 50 µg/mL botanical extract with 2% $AlCl_3$, 1 h incubation, 420 nm detection and sample-blank correction has direct methodological precedent (Anwar *et al.*, 2020). TFC was expressed as mg quercetin equivalents (QE)/g dried extract.

DPPH radical-scavenging assay

DPPH radical scavenging was measured using a methanolic 1,1-diphenyl-2-picrylhydrazyl assay following Ita and Eduok (2022). DPPH solution was prepared by dissolving 33 mg DPPH in 1 L methanol and was protected from light. Extract and ascorbic acid were dosed so that the final operational concentrations in the 6 mL reaction mixture were 10, 50, 100, 250, 500 and 1,000 µg/mL. One millilitre of the appropriately concentrated test solution was mixed with 5 mL DPPH solution, incubated in the dark for 20 min at 27 °C and read at 517 nm. At every extract concentration, a matched extract blank was prepared by replacing DPPH solution with methanol,

following established blank-corrected spectrophotometric practice for pigmented botanical samples (Yeo and Shahidi, 2019; Rattaya *et al.*, 2015; Rengasamy *et al.*, 2012).

Blank-corrected inhibition was calculated as:

$$Inhibition\ (\%) = \left[1 - \frac{(A_s - A_{sb})}{(A_c - A_{cb})}\right] \times 100 \quad (3)$$

In Equation 3, each sample or control term is corrected by subtracting the absorbance of its corresponding matched blank.

Ferric-reducing antioxidant power

FRAP was measured using the Ferric Reducing Antioxidant Power Assay Kit (Sigma-Aldrich MAK369) according to the kit procedure (Sigma-Aldrich, 2019). Ten microlitres of sample or ferrous standard was placed in each well. Ferrous standards were prepared from the 2 mM standard to provide 0–20 nmol/well. The reaction was initiated with 190 µL of reaction mix containing FRAP assay buffer, $FeCl_3$ solution and FRAP probe in a 152:19:19 µL ratio. Parallel extract-background wells contained the corresponding 171:19 µL buffer:$FeCl_3$ mixture without FRAP probe. Absorbance at 594 nm was monitored at 37 °C for 60 min, and the 60-min reading was used. Results were expressed as mM Fe^{2+} equivalents after application of the recorded dilution factor.

Total antioxidant capacity

TAC was determined using the Total Antioxidant Capacity Assay Kit (Sigma-Aldrich MAK187) according to the kit chemistry (Sigma-Aldrich, 2018). Trolox standards were prepared from a 1 mM stock to provide 0, 4, 8, 12, 16 and 20 nmol/well and brought to 100 µL with ultrapure water. A 0.10 µL aliquot of extract was used per sample well. Sample wells were brought to 100 µL and 100 µL of freshly prepared Cu^{2+} working solution (1:49 Cu^{2+} reagent:assay diluent) was added. Plates were incubated for 90 min at room temperature protected from light and read at 570 nm. The zero-Trolox blank and matched extract blank were subtracted before interpolation from the standard curve. TAC was calculated after accounting for sample volume and expressed as mM Trolox equivalents.

Acetylcholinesterase inhibitory activity

AChE inhibition was evaluated using a modified Ellman microplate procedure (Ellman *et al.*, 1961; Dohi *et al.*, 2009; Jazayeri *et al.*, 2014). Ready-to-use assay buffer (Sigma-Aldrich Catalog Number CS0003A) and AChE positive-control solution (Sigma-Aldrich Catalog Number CS0003C) were used as supplied (Sigma-Aldrich, 2025).

For each well, 25 µL extract solution was combined with 50 µL assay buffer and 25 µL AChE solution adjusted to 0.22 U/mL and incubated at 37 °C for 15 min. Then 125 µL of 3 mM 5,5′-dithiobis(2-nitrobenzoic acid) (DTNB) and 25 µL of 15 mM acetylthiocholine iodide (ATCI) were added; the mixture was incubated for 30 min at room temperature and read at 412 nm. Final operational well concentrations were 10, 25, 50, 100 and 200 µg/mL for the extract and 0.5, 1, 2, 4 and 8 µg/mL for galantamine. Each concentration had a matched sample blank without enzyme; control and control-blank wells were processed in parallel, following the same principle used in blank-corrected Ellman assays (Kitazawa *et al.*, 2021). Inhibition was calculated using Equation 3.

GC-MS profiling

Derivatized GC-MS profiling was performed at the Central Instrumentation Facility, De La Salle University, Biñan, Laguna, Philippines, using an Agilent 8890 GC coupled to a 5977B Mass Selective Detector and an HP-5MS capillary column (30 m × 0.250 mm i.d., 0.25 µm film). MassHunter Qualitative Analysis 10.00 was used for data processing and NIST MS Search 2.3 for library matching (Table 1).

Fifty milligrams of dried ethanolic extract was reconstituted in 500 µL methanol:water (50:50, v/v), vortexed for 1 min, sonicated for 5 min and centrifuged at 12,000 rpm for 5 min.

Fifty microlitres of supernatant was dried by centrifugal vacuum concentration.

Methoxyamine hydrochloride in pyridine (20 µL, 30 mg/mL) was added and the sample was heated at 37 °C for 2 h with intermittent shaking. BSTFA

containing 1% TMCS (20 µL) was then added and the mixture was heated at 37 °C for 1 h, followed by 1 h at room temperature before injection. A reagent blank underwent the same derivatization sequence.

GC-MS peak annotations were assigned by NIST-library spectral matching and are reported as putative annotations. Peaks eluting before 5 min were assigned by the analytical laboratory to derivatization reagents and excluded from biological interpretation. Peak area is reported as chromatographic instrument response. Annotation terminology follows established mass-spectral reporting conventions (Schymanski *et al.*, 2014).

Table 1. GC-MS acquisition and data-processing parameters

Parameter	Setting
Injection	1.0 µL; split 1:50
Carrier-gas flow	1 mL/min
Oven program	45 °C → 180 °C at 12 °C/min → 250 °C at 5 °C/min → 300 °C at 10 °C/min; hold 10 min
Total runtime	40.25 min
Ionization	Electron ionization, 70 eV
Acquisition	Scan, m/z 50–550
Software/library	MassHunter Qualitative Analysis 10.00; NIST MS Search 2.3

Statistical analysis

Three independent extraction/assay trials using separately prepared sample batches constituted the experimental replication (n = 3). Trial-level results are presented as mean ± standard deviation (SD), and relative standard deviation (RSD) was calculated to summarize between-trial dispersion. Concentration-response relationships for DPPH and AChE inhibition were fitted by logarithmic regression using operational final concentrations, and goodness of fit was expressed as R^2.

$$RSD\ (\%) = \frac{SD}{\bar{x}} \times 100 \quad (4)$$

For DPPH and AChE concentration-response data, the prespecified logarithmic model was fitted to percentage inhibition as a function of the natural logarithm of operational final concentration, C:

$$y = a\ln(c) + b; \quad IC_{50} = e^{\left[\frac{(0.50-b)}{a}\right]} \quad (5)$$

where y is inhibition expressed as a fraction and C is the operational final concentration in the reaction mixture or well. IC_{50} was calculated from the fitted regression equation at y = 0.50.

RESULTS

Extraction yield and phytochemical indices

The three independent 100-g dried-flower extraction batches yielded 23.70 ± 0.275% dried ethanolic extract, corresponding to an RSD of 1.16% (Table 2).

Phenolic and flavonoid indices and antioxidant capacity

TPC was 117.937 ± 1.074 mg GAE/g dried extract and TFC was 26.418 ± 0.278 mg QE/g dried extract, with RSD values of 0.91% and 1.05%, respectively (Table 2). The extract showed DPPH radical scavenging with an IC_{50} of 113.25 µg/mL based on operational final reaction concentration. The fitted ascorbic-acid response yielded an IC_{50} estimate of 3.69 µg/mL. FRAP was 380.84 mM Fe^{2+} equivalents and TAC was 514.71 mM Trolox equivalents (Table 3).

Acetylcholinesterase inhibition

The dried ethanolic flower extract inhibited AChE with an IC_{50} of 28.44 µg/mL and R^2 = 0.9945. The fitted galantamine response yielded an IC_{50} estimate of 0.39 µg/mL with R^2 = 0.9817 (Table 4; Fig. 1).

GC-MS profile

The blank-subtracted derivatized chromatogram contained 44 NIST library-matched peaks. Six putative annotations with established relevance to antioxidant, lipid or neurobiological pathways were selected for focused interpretation (Table 5). Among these selected peaks, γ-sitosterol showed the largest chromatographic peak area (25,794,547), followed by linoleic acid (14,831,704) and syringic acid (4,888,448).

Table 2. Extraction yield and compositional indices across three independent batches/trials (n = 3)

Parameter	Mean ± SD	RSD (%)
Extraction yield (% w/w)	23.70 ± 0.275	1.16
Total phenolic content (mg GAE/g extract)	117.937 ± 1.074	0.91
Total flavonoid content (mg QE/g extract)	26.418 ± 0.278	1.05

Table 3. Antioxidant assay results for dried ethanolic *Myosotis sylvatica* flower extract

Endpoint	Extract result	Reference/calibration	Fit or unit
DPPH scavenging, IC_{50}	113.25 µg/mL	Ascorbic acid: 3.69 µg/mL*	R^2 0.9676 / 0.9402
FRAP	380.84	Fe^{2+} calibration	mM Fe^{2+} equivalents
Total antioxidant capacity	514.71	Trolox calibration	mM Trolox equivalents

*Ascorbic-acid IC_{50} was obtained from the fitted concentration-response regression.

Table 4. Acetylcholinesterase inhibition based on operational concentrations in the completed microplate well

Sample	IC_{50} (µg/mL)	R^2
Myosotis sylvatica flower extract	28.44	0.9945
Galantamine	0.39	0.9817

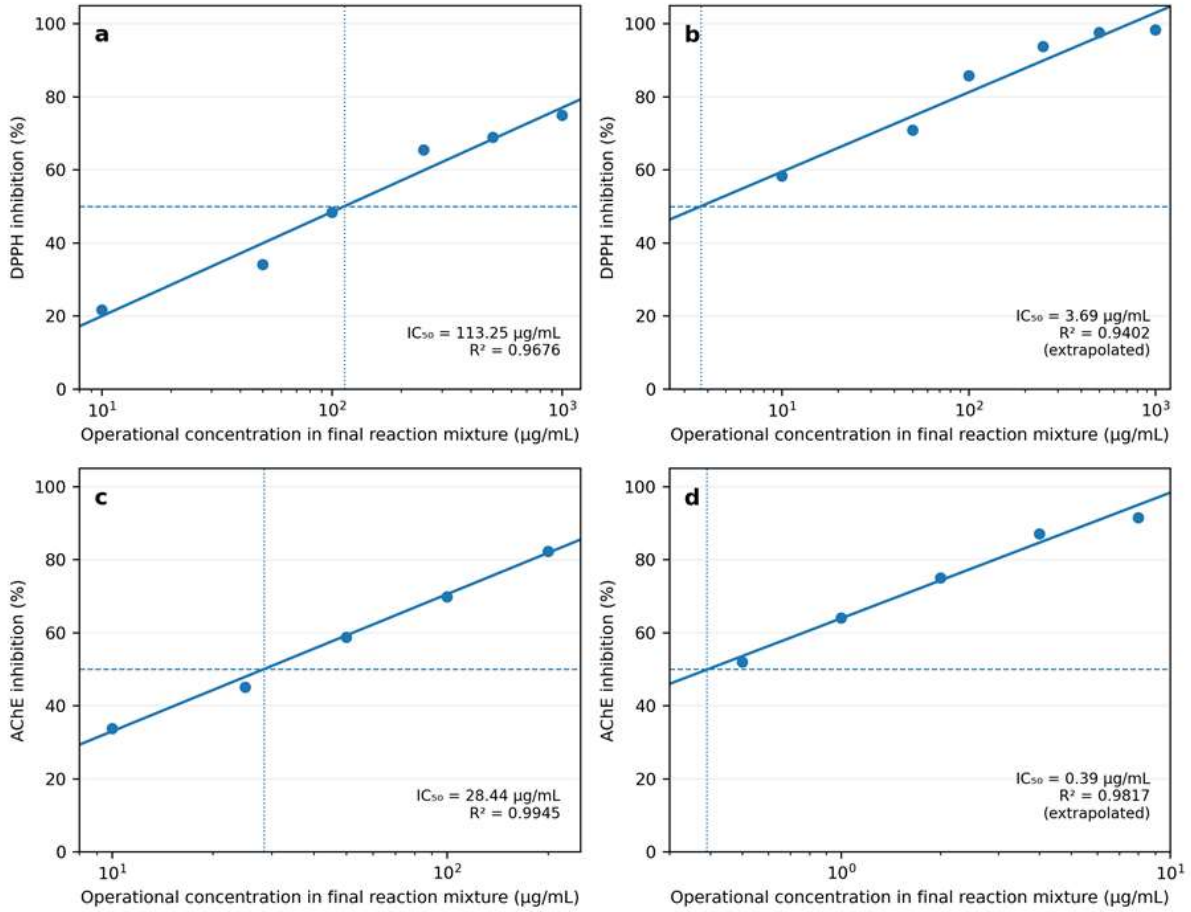


Fig. 1. Concentration-response profiles based on operational concentrations in the completed reaction mixture or well: (a) DPPH scavenging by *Myosotis sylvatica* flower extract; (b) DPPH scavenging by ascorbic acid; (c) AChE inhibition by *Myosotis sylvatica* flower extract; (d) AChE inhibition by galantamine. Dashed horizontal lines indicate 50% inhibition; dotted vertical lines indicate regression-derived IC_{50} estimates

Table 5. Selected biologically relevant putative annotations from derivatized GC-MS

Compound	Class	RT (min)	Peak area	Match	R.Match
Syringic acid	Phenolic acid	15.226	4,888,448	931	967
Phytol	Diterpenoid alcohol	19.564	992,851.1	860	896
Linoleic acid	Polyunsaturated fatty acid	19.878	14,831,704	924	948
Campesterol	Phytosterol	33.119	4,726,244	880	929
Stigmasterol	Phytosterol	33.497	4,434,269	873	894
γ-Sitosterol	Phytosterol	34.248	25,794,547	952	954

DISCUSSION

Extraction yield and phytochemical profile

The dried ethanolic extract yield was 23.70 ± 0.275% across the three independent batches, with an RSD of 1.16%. TPC and TFC likewise showed low between-trial dispersion, with RSD values of 0.91% and 1.05%, respectively. The TPC of 117.937 mg GAE/g and TFC of 26.418 mg QE/g demonstrate substantial recovery of phenolic- and flavonoid-reactive constituents from the flower extract. Recent studies of *Myosotis sylvatica* and *Myosotis amoena* similarly document phenolic constituents and antioxidant-related activity in the genus (Aytar *et al.*, 2026; Yapıcı *et al.*, 2025).

The TFC value of 26.418 mg QE/g complements the TPC result and indicates a measurable flavonoid contribution to the phenolic fraction of the dried ethanolic flower extract.

Aluminium-chloride colorimetry is widely applied for comparative assessment of flavonoid-rich botanical extracts (Madike *et al.*, 2017; Bizuayehu *et al.*, 2016).

Antioxidant profile

DPPH, FRAP and TAC characterize different aspects of antioxidant behavior: radical scavenging, ferric-ion reducing capacity and Cu^{2+}-reducing capacity, respectively (Hidalgo and Almajano, 2017; Munteanu and Apetrei, 2021). The extract showed activity across all three systems, with a DPPH IC_{50} of 113.25 µg/mL, FRAP of 380.84 mM Fe^{2+} equivalents and TAC of 514.71 mM Trolox equivalents. The concordant responses across distinct assay chemistries indicate broad redox activity of the dried ethanolic flower extract. Multi-assay antioxidant evaluation combined with chemical profiling has likewise been applied to plant extracts to relate antioxidant behavior to chemical composition (Padinjarekutt and Saraf, 2024).

The TAC assay yielded 514.71 mM Trolox equivalents under the MAK187 Cu^{2+}-reduction chemistry. In conjunction with the FRAP response, this result shows that the extract contains constituents capable of reducing both ferric and cupric redox systems, complementing the direct radical-scavenging response measured by DPPH.

The DPPH IC_{50} of 113.25 µg/mL confirms concentration-dependent radical-scavenging activity. Recent work on *Myosotis sylvatica* and *Myosotis amoena* also reports antioxidant activity and phenolic constituents, supporting the genus as a source of redox-active natural products (Aytar *et al.*, 2026; Yapıcı *et al.*, 2025).

Acetylcholinesterase inhibition

The extract produced concentration-dependent AChE inhibition with an IC_{50} of 28.44 µg/mL and a strong logarithmic fit (R^2 = 0.9945). Galantamine showed greater potency, with a fitted IC_{50} estimate of 0.39 µg/mL. The magnitude and concentration dependence of the response demonstrate clear cholinesterase-inhibitory activity of the dried ethanolic flower extract.

The AChE response remained evident after concentration-matched blank correction. Similar Ellman-type procedures are used in natural-product cholinesterase screening (Dohi *et al.*, 2009; Jazayeri *et al.*, 2014; Kitazawa *et al.*, 2021). AChE-active flower extracts have been reported for *Nymphaea pubescens*, *Calendula officinalis* and *Tabernaemontana pandacaqui* (Acharya *et al.*, 2018; Olennikov *et al.*, 2017; Athipornchai *et al.*, 2020), while the related

Boraginaceae species *Nonea micrantha* has shown concurrent anticholinesterase, antioxidant and GC-MS profiles (Imran *et al.*, 2017). The present result extends this pattern to *Myosotis sylvatica* flowers.

GC-MS interpretation and candidate constituents

Derivatized GC-MS generated 44 NIST library-matched peaks spanning terpenoid, fatty-acid, hydrocarbon and phytosterol classes. The annotations are reported as putative library matches in accordance with standard mass-spectral reporting practice (Schymanski *et al.*, 2014).

Among the selected biologically relevant peaks, γ-sitosterol, linoleic acid and syringic acid showed the largest chromatographic responses. The selected annotations provide a coherent chemical context for the observed bioactivities.

Phytol has documented antioxidant activity in experimental models (Costa *et al.*, 2016), syringic acid is a phenolic acid associated with antioxidant and neurobiological activities (Srinivasulu *et al.*, 2018), and linoleic acid contributes to neuronal membrane lipid biology (Bazinet and Layé, 2014). Plant sterols have also been investigated in neurotoxicity models (Yadav *et al.*, 2023), while phenolic and other natural-product scaffolds are established sources of cholinesterase-interacting compounds (Işık and Beydemir, 2021; Smyrska-Wieleba and Mroczek, 2023). The predominance of γ-sitosterol among the selected GC-MS peaks, together with linoleic acid and syringic acid, prioritizes these chemical classes for targeted fractionation and confirmatory analysis.

CONCLUSION

Three independent 100-g dried-flower extraction batches yielded 23.70 ± 0.275% dried ethanolic *Myosotis sylvatica* flower extract. The extract consistently exhibited substantial phenolic and flavonoid indices, DPPH radical-scavenging activity, ferric- and cupric-reducing antioxidant capacity, and concentration-dependent AChE inhibition with an IC_{50} of 28.44 µg/mL based on operational final well concentration. Derivatized GC-MS generated 44 library-matched peaks, including γ-sitosterol, linoleic acid, syringic acid, campesterol, stigmasterol and phytol among the biologically relevant putative annotations. The integrated phytochemical, antioxidant, enzyme-inhibition and GC-MS profile supports *Myosotis sylvatica* flowers as a promising source of redox-active and cholinesterase-inhibitory natural products for bioassay-guided fractionation and targeted chemical characterization.

ACKNOWLEDGEMENTS

This research was funded by Partido State University through the Natural Products Research Center. Experimental analyses were conducted at the Bioassay and Potential Drug Screening Research Laboratory, established through Commission on Higher Education Institutional Development and Innovation Grant. GC-MS analysis was performed at the Central Instrumentation Facility, De La Salle University, Biñan, Laguna, Philippines.

REFERENCES

Acharya J, Dutta M, Chaudhury K, De B. 2018. Metabolomics and chemometric study for identification of acetylcholinesterase inhibitor(s) from the flower extracts of *Nymphaea pubescens*. Journal of Food Biochemistry **42(5)**, e12575.

Anwar S, Almatroudi A, Allemailem K S, Joseph R J, Khan A A, Rahmani A H. 2020. Protective effects of ginger extract against glycation and oxidative stress-induced health complications: An in vitro study. Processes **8(4)**, 468.

Athipornchai A, Ketpoo P, Saeeng R. 2020. Acetylcholinesterase inhibitor from *Tabernaemontana pandacaqui* flowers. Natural Product Communications **15(3)**, 1934578X20911488.

Aytar E C, Aydın B, Torunoğlu E I, Durmaz A. 2026. Scent-derived bioactivity of *Myosotis sylvatica* flowers: GC-MS-based volatile profiling and computational evaluation of antioxidant targets. Flavour and Fragrance Journal **41**, 617-627.

Bazinet R P, Layé S. 2014. Polyunsaturated fatty acids and their metabolites in brain function and disease. Nature Reviews Neuroscience **15**, 771-785.

Bizuayehu D, Atlabachew M, Ali M T. 2016. Determination of some selected secondary metabolites and their *in vitro* antioxidant activity in commercially available Ethiopian tea (*Camellia sinensis*). SpringerPlus **5**, 412.

Butterfield D A, Halliwell B. 2019. Oxidative stress, dysfunctional glucose metabolism and Alzheimer disease. Nature Reviews Neuroscience **20**, 148-160.

Chen Z R, Huang J B, Yang S L, Hong F F. 2022. Role of cholinergic signaling in Alzheimer's disease. Molecules **27**, 1816.

Costa J P, Islam M T, Santos P S, Ferreira P B, Oliveira G L S, Alencar M V O B, Paz M F C J, Ferreira E L F, Feitosa C M, Citó A M G L, Sousa D P, Melo-Cavalcante A A C. 2016. Evaluation of antioxidant activity of phytol using non- and pre-clinical models. Current Pharmaceutical Biotechnology **17(14)**, 1278-1284.

Cummings J. 2021. New approaches to symptomatic treatments for Alzheimer's disease. Molecular Neurodegeneration **16**, 2.

Dohi S, Terasaki M, Makino M. 2009. Acetylcholinesterase inhibitory activity and chemical composition of commercial essential oils. Journal of Agricultural and Food Chemistry **57(10)**, 4313-4318.

Ellman G L, Courtney K D, Andres V Jr, Featherstone R M. 1961. A new and rapid colorimetric determination of acetylcholinesterase activity. Biochemical Pharmacology **7(2)**, 88-95.

Gasga K. 2026. Qualitative phytochemical screening of medicinal plants used by Partido Albularyo in Camarines Sur, Philippines. Open Access Library Journal **13**, e15892.

Hampel H, Mesulam M M, Cuello A C, Farlow M R, Giacobini E, Grossberg G T, Khachaturian A S, Vergallo A, Cavedo E, Snyder P J, Khachaturian Z S. 2018. The cholinergic system in the pathophysiology and treatment of Alzheimer's disease. Brain **141**, 1917-1933.

Hidalgo G I, Almajano M P. 2017. Red fruits: Extraction of antioxidants, phenolic content, and radical scavenging determination: A review. Antioxidants **6(1)**, 7.

Imran M, Ullah F, Ayaz M, Sadiq A, Shah M R, Jan M S, Ullah F. 2017. Anticholinesterase and antioxidant potentials of *Nonea micrantha* Boiss. and Reut along with GC-MS analysis. BMC Complementary and Alternative Medicine **17**, 499.

Işık M, Beydemir Ş. 2021. The impact of some phenolic compounds on serum acetylcholinesterase: Kinetic analysis of an enzyme/inhibitor interaction and molecular docking study. Journal of Biomolecular Structure and Dynamics **39**, 6515-6523.

Ita B N, Eduok S I. 2022. In vitro antioxidant and antifungal activities of *Rhizophora racemosa* G.F.W. Mey. stem bark extracts. Scientific African **15**, e01091.

Jazayeri S B, Amanlou A, Ghanadian N, Pasalar P, Amanlou M. 2014. A preliminary investigation of anticholinesterase activity of some Iranian medicinal plants commonly used in traditional medicine. DARU Journal of Pharmaceutical Sciences **22**, 17.

Karim N, Khan H, Khan I, Guo O, Sobarzo-Sánchez E, Rastrelli L, Kamal M A. 2020. An increasing role of polyphenols as novel therapeutics for Alzheimer's: A review. Medicinal Chemistry **16(8)**, 1007-1021.

Kitazawa K, Nagasawa-Shimura N, Tanaka K, Musashi M, Kubota Y, Nagasawa T, Yamaguchi Y. 2021. A novel function of sphingosylphosphorylcholine on the inhibitory effects of acetylcholinesterase activity. Biological and Pharmaceutical Bulletin **44(11)**, 1717-1723.

Knopman D S, Amieva H, Petersen R C, Chételat G, Holtzman D M, Hyman B T, Nixon R A, Jones D T. 2021. Alzheimer disease. Nature Reviews Disease Primers **7**, 33.

Madike L N, Takaidza S, Pillay M. 2017. Preliminary phytochemical screening of crude extracts from the leaves, stems, and roots of *Tulbaghia violacea*. International Journal of Pharmacognosy and Phytochemical Research **9(10)**, 1300-1308.

Moreira N C D S, Lima J E B F, Marchiori M F, Carvalho I, Sakamoto-Hojo E T. 2022. Neuroprotective effects of cholinesterase inhibitors: Current scenario in therapies for Alzheimer's disease and future perspectives. Journal of Alzheimer's Disease Reports **6**, 177-193.

Munteanu I G, Apetrei C. 2021. Analytical methods used in determining antioxidant activity: A review. International Journal of Molecular Sciences **22**, 3380.

Olennikov D N, Kashchenko N I, Chirikova N K, Akobirshoeva A, Zilfikarov I N, Vennos C. 2017. Isorhamnetin and quercetin derivatives as anti-acetylcholinesterase principles of marigold (*Calendula officinalis*) flowers and preparations. International Journal of Molecular Sciences **18(8)**, 1685.

Padinjarekutt D L, Saraf A. 2024. Antioxidant activity study and GC-MS profiling of leaves, stem and root extracts of *Spermadictyon suaveolens* Roxb. Academia Journal of Biology **46(3)**, 37-61.

Phuyal N, Jha P K, Raturi P P, Rajbhandary S. 2020. Total phenolic, flavonoid contents, and antioxidant activities of fruit, seed, and bark extracts of *Zanthoxylum armatum* DC. The Scientific World Journal **2020**, 8780704.

Pisoschi A M, Pop A, Cimpeanu C, Predoi G. 2016. Antioxidant capacity determination in plants and plant-derived products: A review. Oxidative Medicine and Cellular Longevity **2016**, 9130976.

Rattaya S, Benjakul S, Prodpran T. 2015. Extraction, antioxidative, and antimicrobial activities of brown seaweed extracts, *Turbinaria ornata* and *Sargassum polycystum*, grown in Thailand. International Aquatic Research **7**, 1-16.

Rengasamy R R K, Rajasekaran A, Micheline G-D, Perumal A. 2012. Antioxidant activity of seagrasses of the Mandapam coast, India. Pharmaceutical Biology **50(2)**, 182-187.

Scheltens P, De Strooper B, Kivipelto M, Holstege H, Chételat G, Teunissen C E, Cummings J, van der Flier W M. 2021. Alzheimer's disease. The Lancet **397**, 1577-1590.

Schymanski E L, Jeon J, Gulde R, Fenner K, Ruff M, Singer H P, Hollender J. 2014. Identifying small molecules via high resolution mass spectrometry: Communicating confidence. Environmental Science and Technology **48**, 2097-2098.

Sigma-Aldrich. 2018. Total Antioxidant Capacity Assay Kit, Catalog Number MAK187: Technical Bulletin. https://www.sigmaaldrich.com/deepweb/assets/sigmaaldrich/product/documents/273/123/mak187bul.pdf [accessed 12 September 2026].

Sigma-Aldrich. 2019. Ferric Reducing Antioxidant Power (FRAP) Assay Kit, Catalog Number MAK369: Technical Bulletin. https://www.sigmaaldrich.com/deepweb/assets/sigmaaldrich/product/documents/368/820/mak369bul.pdf [accessed 12 September 2026].

Sigma-Aldrich. 2025. Acetylcholinesterase Activity Assay Kit (Colorimetric), Catalog Number CS0003: Technical Bulletin, Rev. 9/25. https://www.sigmaaldrich.com/deepweb/assets/sigmaaldrich/product/documents/312/814/cs0003bul-ms.pdf [accessed 12 September 2026].

Smyrska-Wieleba N, Mroczek T. 2023. Natural inhibitors of cholinesterases: Chemistry, structure-activity and methods of their analysis. International Journal of Molecular Sciences **24**, 2722.

Srinivasulu C, Ramgopal M, Ramanjaneyulu G, Anuradha C M, Suresh Kumar C. 2018. Syringic acid (SA)-a review of its occurrence, biosynthesis, pharmacological and industrial importance. Biomedicine and Pharmacotherapy **108**, 547-557.

Wang F, Miao M, Xia H, Yang L G, Wang S K, Sun G J. 2017. Antioxidant activities of aqueous extracts from 12 Chinese edible flowers in vitro and in vivo. Food and Nutrition Research **61**, 1265324.

Yadav S, Aggarwal P, Khan F, Khodve G, Padhy D S, Yadav P, Banerjee S. 2023. β-Sitosterol protects against aluminium chloride-mediated neurotoxicity. Current Alzheimer Research **20(1)**, 29-37.

Yapıcı İ, Kayaoğlu E, İzol E, Yilmaz M A, Behçet L, Cakır O, Gülçin İ. 2025. Phytochemical profile, antioxidant capacity, acetylcholinesterase, and butyrylcholinesterase enzyme inhibition properties of *Myosotis amoena* Boiss. Chemistry and Biodiversity **22(12)**, e02157.

Yeo J, Shahidi F. 2019. Critical re-evaluation of DPPH assay: Presence of pigments affects the results. Journal of Agricultural and Food Chemistry **67(26)**, 7526-7529.